Study Case: Electromechanical Design of a Magnetic Damper for Robotic Systems

Guillermo Enrique Fúnez, Alberto Max Carrasco, and José Luis Ordoñez-Ávila
Universidad Tecnológica Centroamericana (UNITEC), San Pedro Sula, Honduras
Email: guienfuca96@unitec.edu, alberto.carrasco@unitec.edu.hn, jlordonez@unitec.edu

***Abstract*—Robots are entering the technological age giving way to endless applications in the automation industry. Robots of different applications need suspensions systems to perform their logistic or agro-industrial activities. The aim is to design a mechanical vibration damping device that uses the principles of electromagnetism in order to control the magnetic viscosity, and thus the way it can absorb vibrations that are undesirable in robotic systems. This research project has a complete theoretical framework and quantitative approach to determining variables and measuring the response at the experimental and mathematical level. The theoretical framework explains the bases for the mathematical model. The method was based on five stages which are design specifications, preparation of schematics, electrical and mechanical tests, mechanical and electrical part coupling and prototype test. As key facts, a physical and mathematical model were designed for a shock absorber device with magnetic principles for robotic systems. The electric current of 1.6 A and a permeability of material 5001 are key variables that result in a damper magnetic viscosity γ = 7.32 T.m. Finally, authors conclude magnetic dampers can be used in unmanned robots allowing them to save energy on flat surfaces.**

***Index Terms*—automation industry, irregular terrain, principles of electromagnetism & damping**

I. Introduction

Robotics is a multidisciplinary science involving electronics, artificial intelligence systems, mechanics, and control systems. Today it has had a high impact on the automation industry, solving problems in production lines, agribusiness, space sciences, among others. It plays a crucial role in performing complex or repetitive tasks, making it feasible for almost any application that requires it. Suspension systems are critical because they absorb some of the energy during impacts or when entering uneven terrain, that energy converts it into heat energy. This prevents movements in the system from being abrupt, compromising the electronic equipment to such shocks, and maintaining linearity while moving [1].

By applying the theories of electrical and magnetic principles, it is possible to design a damping system based on these phenomena. They are allowing it to be hybrid and maintaining control of the dampers using the robot's instructional commands. This reduces current consumption and always keeps the coil spring system activated [2]. The purpose of these systems is to significantly reduce the amplitude of mechanical vibration on the rebounds of the mass of the vehicle, allowing to balance it with a noble and smooth movement. The operation is governed by some fundamental theorems of electromagnetic physics [3]. The model of this study consists of an inductor that has a steel core and a coil spring.

II. Theoretical Framework

A. Electromechanical Suspension System

The mechanical suspension consists of a spring, which is responsible for storing potential energy during any impact or irregularity, the damper dissipates mechanical energy in heat employing a viscous fluid. The mass preserves the kinetic energy of the system. Currently, in robots, these mechanisms are used to reduce vibrations. The electromagnetic actuator systems with inductors and springs are also used in order to eliminate disturbances. This allows to control the precise moments when mechanical damping requires giving it freedom during the immobility of the robot or in places where it does not require it [4].

In the system, a fluid damper is changed to a magnetic one, which is connected to the robot controller and can be activated or disabled. Equation 1 describes the movement.

$$m\ddot{x} + \Upsilon\dot{x} + kx = 0 \quad (1)$$

This is the mathematical representation in differential equations of a conventional mechanical suspension system, where m is the total *mass*, ϒ is the coefficient of magnetic viscosity, and k is the Constant of Hook in the spring. This mathematical representation was adapted to replace an electromagnetic damper. For this, it is required to define a value for the constate of magnetic viscosity. This magnetic viscosity appears in the core as a result of opposition to the movement.

B. Electrical and Magnetic Principles

The physical foundations governing magnetic behavior can be used to take control of components electrically, taking advantage of such phenomena.
This design is based on Ampere's law, which establishes the postulate of magnetostatics. This magnetostatics involves magnetic flux density B and electric current I that

Manuscript received July 5, 2021; revised November 1, 2021.

doi: 10.18178/ijmerr.11.2.66-72

passes through a given conductive medium as in equation 2.

$$\oint \vec{B} \cdot d\vec{l} = \mu I \tag{2}$$

For design, *B* is defined as the magnetic flux density through a dl *boundary*.

$$\vec{B} = \vec{B}_z \cdot \hat{k} \tag{3}$$

$$d\vec{l} = dz \cdot \hat{k} \tag{4}$$

By solving the integral that passes through the contour. The magnetic flux density is obtained through the nucleus with both air and ferromagnetic material permeabilities, resulting in simplified in equation 4.

$$\vec{B}_z = \frac{\mu N i}{z} \hat{k} \tag{5}$$

Viscosity is related to some opposition to the movement when a core of ferromagnetic material moves within an electromagnetic field experiencing a force that depends directly on the magnetic permeability and intensity of this field. An equation is established for magnetic viscosity respecting the principles of Ampere's law and the Newtonian equation, which relates speed to the force he exerts [5].

C. Inductance

Just as a capacitor stores energy in the form of electric fields, the inductor does so through a magnetic field that can vary depending on the geometry of the magnetic field. In the study of magnetic damping based on the solenoidal model. The inductance is the way to calculate the force exerted by the damper; this depends on the intensity of the magnetic field produced [6]. Circulating an electrical current in an inductor generates an H-intensity magnetic field that has two poles and tends to align the magnetic domains of the materials [7]. To obtain the inductance, the flow must be obtained through the core surface defined in equation 6.

$$\phi_z = \int \vec{B} \cdot d\vec{s} \tag{6}$$

The core has a cylindrical geometry, and the flow that crosses that cross-section is expressed the integral of this. Equation 5 is replaced for the final expression.

$$d\vec{s} = r dr d\theta \tag{7}$$

$$\phi_z = \iint_0^R \frac{\mu N i}{z} \cdot r dr d\theta \tag{8}$$

$$\phi_z = \frac{\mu \pi N I R^2}{z} \tag{9}$$

Inductance is defined in equation 10.

$$L = \frac{\lambda_{11}\phi_z}{I} = \frac{\mu \pi N^2 R^2}{z} \tag{10}$$

Inductance is the ability of an inductor to store that magnetic energy with the unit in Henry. This unit, as inductance, is observed, it has the independence to the current, so this value is a constant in most applications.

D. Work and Magnetic Force

Magnetic work follows the concept of the amount of energy a body needs to move a particle from point A to point B, it is implicitly involved with inductance, since it was mentioned that it is a way of storing energy and in this study, it is of importance to determine the forces that the nucleus has to move in a mechanical oscillation. The work is expressed in equation 11.

$$W_m = \frac{1}{2} L I^2 \tag{11}$$

In this way, it is possible to calculate the partial derivative on the z-axis of the stored magnetic energy and obtain in our model a force adjusted to the design parameters.

$$\vec{F}_z = -\frac{\partial W_m}{\partial z} = -\frac{\partial}{\partial z}\left(\frac{\mu \pi N^2 I^2 R^2}{2z}\right) \tag{12}$$

$$\vec{F}_z = \frac{\mu_o \pi N^2 I^2 R^2}{2z^2} \hat{K} \tag{13}$$

In the designed model, a very intense magnetic field is generated in the center of the core. This magnetic field makes the material manufacturing with high permeability is attracted and always towards the center [8]. In this case, the force experienced by the nucleus is with respect to the vacuum surrounding it, and it is the reason why in equation 13, only air permeability is considered.

E. Magnetic Permeability

All materials have magnetic properties, some weaker than others when magnetic fields are applied. The materials align their molecules to that field, and this causes a magnetic dipolar moment, and this determines the permeable capacity it possesses. Some materials are almost unchanged or imperceptible, classifying them as diamagnetic and ferromagnetic. In most engineering applications, ferromagnetic materials are used, which form a nucleus that is excited by an inductor [9]. For permeabilities, it is established that the reference is that of the vacuum denoted as $\mu_{o.}$ The absolute permeability is described as the product of the relative, in equation 12.

$$\mu = \mu_o \mu_r \tag{12}$$

Based on this concept, a cylindrical iron core that has a permeability of 5000 was chosen for the damper design. Making it possible for magnetic viscosity, which is later explained, to increase significantly and generate an excellent damping effect.

F. Electrical Resistance in Inductors

For the design of a magnetic damper based on the solenoidal principle, the conductors and their environment must be considered. The physical principles of conductance are related to the ability to conduct electrical currents through a cross-section of a conductor. This ratio means that as the cable length increases, the resistance also increases and is expressed in equation 13.

$$R = \rho \frac{l}{A} \tag{13}$$

A hollow cylindrical geometry was chosen, so to calculate the number of turns of enameled copper and the expected resistance should be considered the diameter and length of the cable, that is why for the model of this damper an equation is developed to determine the length of the copper as the perimeter of the cable increases in the winding.

$$dl = 2N\pi \int_{ro}^{rf} dr \tag{14}$$

$$l = 2N\pi(r_f - r_i) \tag{15}$$

From this definition equation, 15 is established to determine the length of the cable winding and thus correspond to a substitution in equation 13, which has a dependency on the area of the cross-section of the copper to be used (this according to the current capacity in the design) and ρrepresenting resistivity, which is the inverse of conductivity.

For the construction of the physical inductor, the variables to be considered in the previous model are denoted. The reason why the inductor resistance should be included is to achieve intensifying the current and with this the magnetic field, using the ohm law to calculate the current that is desired to circulate through it. Having replaced equation 15 in 13, the model is expressed in equation 16.

$$R = \frac{2\rho N(r_f - r_i)}{r^2} \quad [\Omega] \tag{16}$$

Performing a clearing for N representing the number of copper cable turns; this variable is necessary for the manufacture of the damper. In the design, R is replaced by the resistance that is desired, causing it to circulate through the inductor a current, being expressed in equation 17.

$$N = \frac{Rr^2}{2\rho(r_f - r_i)} \tag{17}$$

G. Magnetic Viscocity

The concept of viscosity relates opposition to the movement of a body. This is indicated in equation 18. In a solenoid the magnetic flux increases in the core of the winding and therefore there is the higher magnetic field intensity of the system, when a nucleus of ferromagnetic material of high permeability of about, it increases the force of attraction towards the center, always trying to align itself, therefore, the nucleus when leaving its center of attraction experiences a force of opposition, behaving like an incompressible fluid [10].

$$F = -\Upsilon \frac{dz}{dt} \tag{18}$$

Υ is the magnetic viscous damping coefficient for our model, using this physical concept we develop a mathematical equation that explains the operation of opposition to the movement, based on the damping model of two plates pay them with a fluid, adapts to the design of the magnetic damper expressed in equation 19.

$$\gamma = \frac{A}{h}\vec{B} \tag{19}$$

$$\gamma = \frac{\mu A}{h}\vec{H} \tag{20}$$

For the magnetic viscous damping coefficient, a dependence on magnetic flux density through the medium or media that have absolute permeability in its environment is seen. Where the magnetic permeability to be considered will be that of the air and ferromagnetic material to be used to be constructed, expressed in equation 21.

$$\mu = \mu_o(1 + \mu_r) \tag{21}$$

Leaving as a result of a more robust expression dependent on materials and air, in equation 22.

$$\gamma = \frac{\mu_o(1+\mu_r)\,A}{h}\vec{H} \tag{22}$$

Fig. 1 shows the variables considered as the shock model. By substituting the magnetic field intensity in equation 22 and adapting it to the model in Fig. 1, a unified equation of the magnetic damping coefficient, set out in equation 23, is obtained.

$$\gamma = \frac{\mu_o(1+\mu_r)(2\pi rl)}{2h}\left(\frac{Ni}{l}\right) \tag{23}$$

$$\gamma = \frac{\mu_o(1+\mu_r)\pi rNi}{h} \tag{24}$$

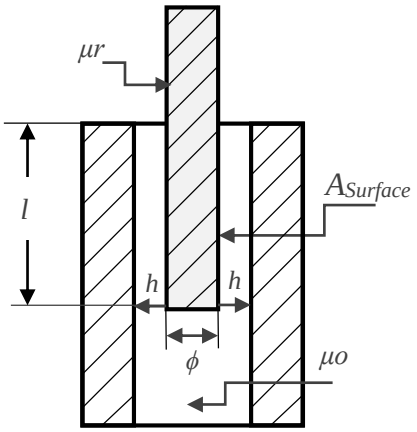

Figure 1. Physical model of magnetic shock absorber

The magnetic damping coefficient is expressed in equation 24 as a design model to make its operation more generic, explaining the phenomenon of opposition to movement dependent on two key variables, the electric current and the permeability of the materials.

H. The Helical Spring

All mechanical systems that aim to absorb the energy of vibrations are accompanied by elements that fulfill specific tasks in the dissipation of these energies. The coil spring or spring has the function of storing the potential energy of an oscillating vibrating system. Such energy is delivered to the shock that meets the dissipation of this energy in the form of heat or other forms of energy. In the magnetic damping model, this mechanical element is elemental, as its rigidity helps to significantly reduce the oscillating movements so undesirable in any robotic system. To perform the system, its design is considered to attach it to it, by means of equation 25.

$$K = \frac{Gd^4}{8nD^3} \tag{25}$$

The stiffness constant of a spring determines the force needed to deform it, thus influencing the oscillating kinematic analysis, preventing all force from resting on the damper. This equation involves variables of utmost importance for the design, considering the rigidity module of the G-spring material, the diameter of the d wire, the mean diameter D, and the number of active turns of the n wire.

I. Mechanical Vibration Control Systems

Engineering control systems allow us to visualize how mechanical systems behave and, based on it, making decisions to make results more efficient.

Magnetic damping behaves like viscous damping through the magnetic flux density and the surrounding medium. In this model, it is a focus of study in mechanical vibrations, where the relationships between mass, spring, and shock must be considered. This is calculated the damping ratio where the mass and spring are involved with the damping by means of equation 26.

$$\delta = \frac{c}{2\sqrt{km}} \tag{26}$$

This relationship allows us to determine whether the responses to the system are complex or real, indicating whether the system is under-damped, critically damped, over-damped, or undamped. This can be expressed as the exponential decay of the sine oscillation, see equation 27.

$$z(t) = e^{-s\omega t}(\acute{c}_1 \cos(\sqrt{1-s^2})\omega t + \acute{c}_2 \sin(\sqrt{1-s^2})\omega t) \tag{27}$$

This relationship expresses the exponential decay of the system before a natural damping frequency, which is described in equation 28. The product *ss s represents* the actual part of the roots calculated for this sub-damped system.

$$\omega = \sqrt{\frac{k}{m}} \tag{28}$$

The natural frequency makes a clear dependence on the two elements that constitute oscillating nature, mass, and spring, the constant of rigidity that obeys Hooke's law.

The above variables make clear implications in control systems. For this reason, it must be seen as a transfer function, where the block is a standard model to replicate this magnetic damper. The expression that is set for frequency mastery and future time analysis in equation 29 and this is due to Newton's second law.

$$F = m\frac{d^2z}{dt^2} + \Upsilon\frac{dz}{dt} + kx \tag{29}$$

This equation is evaluated with the functions of the Laplace transform to establish it in the frequency domain resulting in equation 30.

$$F(u) = m[s^2x(s)] + \gamma[s\,x(s)] + k\,x(s) \tag{30}$$

$$X(s) = \frac{F(u)}{mS^2+\gamma S+k} \tag{31}$$

III. METHODOLOGY

The design of a shock absorber with magnetic qualities requires an exhaustive physical-mechanical analysis to validate its operation. This research project has a quantitative approach to determining variables and measuring the response at the experimental and mathematical level.

Stage I. *Design Specifications:* This section performs a specification collection for the mechanical and electrical design of the device through sustainment theories.

Stage II. *Preparation of schematics:* Mechanical schemes are made, and the electromagnetic variables that will govern the operation of the device through mathematical explanations are studied.

Stage III. *Electrical and mechanical tests*: Small test prototypes are created at this stage and are vital in moving to the next stage and adjusting the design specifications.

Stage IV. *Mechanical and electrical part coupling:* After the evaluation of the stages, both parts are integrated into a valid and functional model for the magnetic damper.

Stage V. Prototype: a prototype is made based on the specifications of the methodology, as a core of evaluation and validation of the operation of the shock after optimal results.

IV. RESULTS AND ANALYSIS

A. Physical and Mathematical Analysis of the Electrical Phenomenon

Considering the principles of operation in the magnetic damper and based on the postulates of the magnetostatics, the idea was merged by the specifications set out in the methodology, and the equations were developed that helped to understand the magnetic behavior in the materials, giving gap to improve the model.

Having described equation 13, the authors note the dependence of the current and the number of turns of copper cable, which is why equations 15 and 16 obtain the electrical resistance by the number of turns, allowing us to manipulate it to increase or decrease the current that will pass through the inductor. Figure 2 for winding uses a radio tube r_i = 0.0065 m and r_f = 0.0175 m.

Figure 2. Top of the copper coil turns

$$N = \frac{(14\,\Omega)(0.2275mm)^2}{2\left(0.0175\frac{\Omega.mm^2}{m}\right)(0.01744-0.0065)m} \tag{32}$$

$$N = 1890.67 \text{ turns}$$

It has been considered a copper cable #25 because its cross-section supports 1.6 amps by having a resistance of 14 and a voltage of 22. Ω50volts, this current is supported by the mentioned caliber. Applying ohm law is obtained.

$$I = \frac{V}{R} = \frac{22.50v}{14\,\Omega} = 1.6\,A \tag{33}$$

Subsequently, the density of magnetic flux was calculated through certain ferromagnetic materials, these

being optimal for the development of the project, due to its high magnetic permeability, through the equation the vector with unit direction is calculated on the z-axis, set in equation 5, equation 32 is obtained.

$$\vec{B} = \frac{\left(4\pi x10^{-7}\frac{T.m}{A}\right)(5000+1)(1890\ turns)(1.6\ A)}{0.0254\ m}\ \hat{K} \quad (34)$$

$$\vec{B} = (752.87\ T)\ \hat{K}$$

This magnetic flux density indicates that for a current of 1.6 amps, there is a flow of 752.86 T through the faces of the iron core with impurities that has a relative permeability of 5000, this is an indicator of increasing magnetic viscosity.

In reference to equation 13, the force experienced by the nucleus is obtained with respect to the void around it.

$$\vec{F}_z = \frac{\pi\left(4\pi x10^{-7}\frac{T.m}{A}\right)(1890.67 turns)^2(1.6A)^2(0.00635m)^2}{2(0.0254m)^2} \quad (35)$$

$$\vec{F}_z = (-1.12\ N)\ \hat{K}$$

In the prototype developed under these conditions, the negative sign determines that it is opposite to the natural harmonic movement of the nucleus, pes this is always attracted to the center of the inductor, where the magnetic field is intense.

For the magnetic viscosity coefficient, a mathematical model is established that generalizes key variables to increase the rigidity in the natural response of an oscillation that is generated by mechanical vibration in a robotic system. Equation 24 raised a clear dependence on the current and the relative permeability of which the core is built.

$$\gamma = \frac{\left(4\pi^2 x10^{-7}\frac{T.m}{A}\right)(5001)(0.003175m)(1890.67\ v)(1.6A)}{0.0254\ m} \quad (36)$$

$$\gamma = 7.32\ T.m$$

This model was plotted as validation of the real results, which indicates that there is linearity between the magnetic viscosity coefficient and the current circulating through the inductor, which makes sense because by increasing the viscosity, the magnetic field is more intense in the damper.

B. Mechanical Vibration Analysis

All dynamic systems suffer deformations that lead to the bodies oscillating generating mechanical vibrations, these are undesirable in any mechanism, because this energy unbalances the bodies causing them to leave their center of gravity suffering high impacts. Shock absorbers and springs serve the function of dissipating mechanical energy in heat. To predict the response of the mechanical system, the damping ratio that is defined by equation 26 was calculated. For this prototype a mass of 200 grams and a spring with stiffness constant of 490 N/m was chosen replacing the magnetic viscosity coefficient:

$$\delta = \frac{7.32}{2\sqrt{(0.2\ Kg)(489.31\ N/m)}} \quad (37)$$

$$\delta = 0.352$$

This value allows us to express an equation with exponential decay through the roots, clarifying that being less than one the system behaves sub-muffled and has complex roots and is defined as:

$$s1 = \left(-\delta \mp \sqrt{\delta - 1}\right)\sqrt{\frac{k}{m}} \quad (38)$$

$$s_{1,2} = \left(-0.352 \mp \sqrt{0.352 - 1}\right)\sqrt{\frac{489.31\ N/m}{0.2\ Kg}} \quad (39)$$

$$s_{1,2} = (-16.6 \mp j\ 37.96) \quad (40)$$

The roots have a complex number. Therefore, to establish a control model, the original part is taken, and values are imposed as indicated in equation 27, leaving a mathematical representation of the physical behavior of the magnetic damper, see equation 41.

$$z(t) = e^{-16.6t}(\grave{c_1}\cos(46.29\ t) + \grave{c_2}\sin(46.29t) \quad (41)$$

Constants C1' and C2' are determined under the initial system conditions, which are:

$$C_1' = x_o = -7.46x10^{-3}m \quad (42)$$

$$C_2' = \frac{\dot{x}_1 + \delta w x_o}{\sqrt{1-\delta^2}w} = 0\ m \quad (43)$$

The final expression is an equation of the time-dependent position, which is a generic model for such vibratory systems; it helps us determine what the final elongation of exponential decay is.

$$z(t) = e^{-16.6t}(-7.46x10^{-3}\cos(46.29\ t)) \quad (44)$$

Using Matlab software, it was possible to predict the natural response of the system where it is clearly evident that the damping ratio by being closer to 1 would dampen the test load on the prototype and by disconnecting the shock, its response is free and unwanted in uneven terrain. It was used for the right graph and δ 7.32 for the left.

For the analysis of the response, the exponential decay of the position is displayed by equation 45, where only the coefficient of the exponential equation is represented.

$$z(t) = x_o e^{-s\omega t} \quad (45)$$

$$z(t) = (-7.46x10^{-3})e^{-16.6t} \quad (46)$$

By evaluating different damping ratios in equation 45, you get a pattern of graphs, which demonstrate comparative deform, that by manipulating key variables such as the current, it is possible to reduce the elongation of the response. These values change depending on the proportionality of the mass and the stiffness constant of the spring, for this reason by equation 25, the constant that follows Hooke linearity was calculated:

$$K = \frac{\left(80.8x10^9\frac{N}{m^2}\right)(0.00079375m)^4}{8(4\ vueltas)(0.0127m)^3} \quad (47)$$

$$K = 489.31\frac{N}{m} \quad (48)$$

Once the prototype specifications have been established, equation 46 was inserted into Matlab obtained from the graphs in Fig. 3.

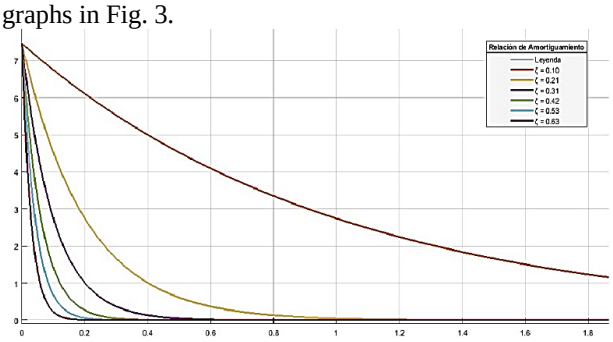

Figure 3. Comparison of stability graphs of the mechanical system.

Such mathematical predictions are attributed to the theoretical model and coincide by validating its operation. In the prototype model is disconnected the shock, then acts as a natural frequency response without viscosity, see Fig. 4, In the prototype and vibration analysis the Tracker software is used, which shows the results concerning the position time, speed and acceleration of the test mass. Subsequently in the prototype test model is applied to a current of 1.6 amps, which according to the theoretical models, would show a sub-muffled response in the system, stabilizing the mass in 1.5 seconds.

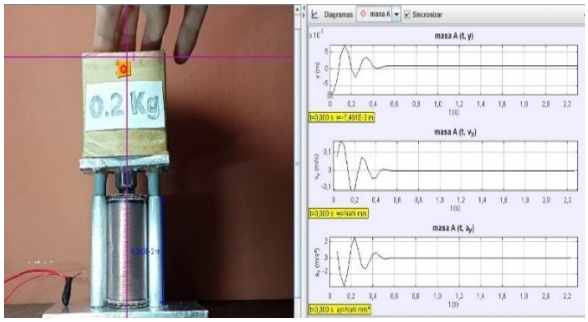

Figure 4. Mechanical vibration analysis of the damped system

C. Modeling Mechanical and Electrical Control Systems

Control models are guidelines that allow you to manipulate critical variables in any system and help visualize changes and make decisions based on the results displayed in a generalized model. The mechanical and electrical system designed in this document has three important global variables in design, magnetic viscosity coefficient, spring stiffness constant and mass, such components can be represented by matrices in a state equation that shows an improved picture of changes.

Since any robotic system has different masses and operating conditions, it must undergo constant testing until the optimal result is obtained for the performance of the joint components. Based on equation 31, we adopt the values for the test model in equation 49.

$$X(s) = \frac{1}{0.2\,S^2+7.32\,S+489.31} \tag{49}$$

The position of the mass is expressed in the frequency domain can be represented in a block diagram as the transfer function. Taking the coefficients of the Laplace transform equation, it is possible to raise state equations.

The operation of the entire system follows Newton's second law, where a differential equation of the second-order, expressed in equation 1, appears. To set the state arrays, you must define state variables and differentiate them for the time to clear for high power. In this case, acceleration can be understood to create a block diagram.

$$\begin{matrix} x_1 = x & \dot{x_1} = \dot{x} \\ x_2 = \dot{x} & \dot{x_2} = \ddot{x} \end{matrix} \tag{50}$$

It clears from equation 1, for acceleration this term that makes expressing the equation more simplicity and being able to understand the changes due to the fundamental values.

$$\ddot{x} = \frac{1}{m}(F(u) - \Upsilon\dot{x} - kx) \tag{51}$$

Using an array of state variables, you can construct a block diagram in the pesto time domain that is modeling the equation differential terms, which is raised in equation 52.

$$\begin{bmatrix} \dot{x}_1 \\ \dot{x}_2 \end{bmatrix} = \begin{bmatrix} 0 & 1 \\ -\frac{\Upsilon}{m} & -\frac{k}{m} \end{bmatrix} \begin{bmatrix} x_1 \\ x_2 \end{bmatrix} + F(u) \begin{bmatrix} 0 \\ \frac{1}{m} \end{bmatrix} \tag{52}$$

Having validated the results after experimental and theoretical tests. The prototype was designed based on the same tests, thus considering the critical variables in the inductor and mechanical design, obtaining a result through this study. The model was created in the SolidWorks software, see Fig. 5.

Figure 5. Block diagram based on the array of states

V. Conclusions

A progressive digital methodology is applied to integrate mechanical and electrical components into a functional and experimental model. A physical and mathematical model is designed for a shock absorber device with magnetic principles for robotic systems. They were modeled with theoretical and experimental tests results of performing the magnetic damper adapting the specifications for modern robotic systems. This model can be used in projects such as [11-12] to get better performance in logistic and agro-industrial applications.

Conflict of Interest

Authors declare there is no conflict of interest.

AUTHOR CONTRIBUTIONS

Guillermo Funez and Jose Luis Ordoñez-Avila conducted the research and wrote the paper. Alberto Max Carrasco provided scientific advisory of this paper; all authors had approved the final version.

REFERENCES

[1] S. Mirzaei, "A flexible electromagnetic damper," *IEEE International Electric Machines & Drives Conference, Antalya*, pp. 959-962, 2007.

[2] A. F. Jahromi and Y. A. Zabihollah, "Application of quadratic linear regulator and fuzzy controller in full car model of magneto-rheological damper suspension system," in *Proc. ASME 2010 on Integrated and Mechatronic Systems and Applications*, Qingdao, 2010

[3] M. Sasaki, J. Kimura, and T. Sugiura, "Vibration suppression in High-Tc superconducting levitation system utilizing nonlinearly coupled electromagnetic shunt damper," in *Proc. IEEE Transactions on Applied Superconductivity*, vol. 25, no. 3, pp. 1-5, June 2015.

[4] M. Yoda and Y. Shiota, "A electromagnetic actuator for a robot working with a man," in *Proc. 1994 3rd IEEE International Workshop on Robot and Human Communication*, Nagoya, Japan, 1994.

[5] A. Fow and M. Duke, "Active electromagnetic damping for lightweight electric vehicles," in *Proc. 2015 6th International Conference on Automation, Robotics and Applications (ICARA)*, Queenstown, 2015.

[6] H. Zhongming, Y. Kai, Z. Xiaowen, Y. T. Xinmin, "Design and experimental study on the MR shock absorber," in *Proc. Third International Conference on Information and Computing, Wuxi, 2010*.

[7] B. Q. Kou, C. M. Zhang, B. P. Yan, and H. C. Cao, "Análisis de la fuerza de detención y supresión del amortiguador eléctrico," *IEEE Vehicle Power and Propulsion Conferencie*, Harbin, 2008.

[8] R. A. Oprea, M. Mihailescu, AI Chirila e ID Deaconu, " Design and efficiency of linear electromagnetic dampers," in *Proc. 13th International Conference on Optimization of Electrical and Electronic Equipment (OPTIM)*, Brasov, 2012.

[9] K. Su and W. Pan, "Design of adaptive fuzzy magnetic suspension vibrator for foot robot," *International Conference on Fuzzy Theory and Its Applications (iFUZZY)*, Yilan, 2015.

[10] V. Dwivedi, A. Kaushal, R. K. Singh, y A. Kumar Sharma, "Analysis of an adaptive vibration absorber in robotics using ferrofluid," in *Proc. 2020 International Conference on Contemporary Computing and Applications (IC3A)*, Lucknow, India, 2020.

[11] J. L. O. Avila et al., "Study case: Teleoperated voice picking robots prototype as a logistic solution in Honduras," in *Proc. 2020 5th International Conference on Control and Robotics Engineering (ICCRE)*, 2020, pp. 19-24.

[12] J. L. O. Avila, H. F. Jimenez, and A. M. Carrasco, "Spiral cycle implementation for designing an all-terrain teleoperated robot in Honduras," in *Proc. 2020 6th International Conference on Robotics and Artificial Intelligence (ICRAI 2020)*. Association for Computing Machinery, New York, NY, USA, 2020, pp. 253–257.

Guillermo Funez is from San Pedro Sula, Cortés, Honduras, graduated as B.Sc. Mechatronics Engineering from UNITEC San Pedro Sula. He currently working in the harness industry in San Pedro Sula Honduras. His major field of study is mechatronic product development. He has design robots and actuators for experimental research. He was recognize as best presentation in his final carreer project.

José Luis Ordoñez Avila, originative Originative from Tegucigalpa, Francisco Morazán, Honduras, is currently a faculty member at UNITEC San Pedro Sula. He is a B.Sc. Industrial Engineering from the USAP, B.Sc. Electronic Engineering from UTH, earned his M.Sc. Project Administration at UNITEC San Pedro Sula. He is member of the Colegio de Ingenieros Mecánicos, Eléctricos y Químicos de Honduras (CIMEQH). His major field of study is robotic applications.
He currently works as professor in the Central American Technological University (UNITEC). He has previously worked as a Project Automation Engineer, and in the design, cost estimation and construction of automation and control system projects. Some of his latest publications are: Robotic wheel structures and their industrial applications based on motion simulations (2021), Design of an Underwater Robot for Coral Reef Monitoring in Honduras (2021), Seven Degrees of Freedom Simulation Comparison for Industrial Process in San Pedro Sula, Honduras (2020). His current and previous research interests are Mechatronic Design applied to robotic systems in Honduras. In 2020 Jose Luis was invited to ICMEAE as session chair and in 2021 he receive the award of best presentation in the same conference.

Alberto Max Carrasco, was born in San Pedro Sula, Honduras on August 17th 1985. Alberto holds a BSc in Mechatronics Engineering from UNITEC, he studied in San Pedro Sula Honduras and graduated in 2008. He later obtained a Master's Degree in Mechatronic Systems from the University of Brasilia, in Brazil in 2013. His major fields of study are mechatronic product development and mechatronic systems models.
He currently works as the Academic Head of the Mechatronics Engineering Program at the Central American Technological University (UNITEC). He also works as a lecturer in the same University. He has previously worked as a Project Automation Engineer, and in the design, cost estimation and construction of automation and control system projects. Some of his latest publications are: Spiral Cycle Implementation for Designing an All-Terrain Teleoperated Robot in Honduras (2020), Study Case: Teleoperated Voice Picking Robots prototype as a logistic solution in Honduras (2020), Low-cost Robot Assistance Design for Health Area to Help Prevent COVID-19 in Honduras (2020) and Face Recognition and Temperature Data Acquisition for COVID-19 Patients in Honduras (2020). His current and previous research interests are Mechatronic Design, Industrial Automation and Control Systems.the biography.